Violation of Local Detailed Balance Despite a Clear Time-Scale Separation

David Hartich[1,*] and Aljaž Godec[1,†]

[1] *Mathematical bioPhysics Group, Max Planck Institute for Biophysical Chemistry, 37077 Göttingen, Germany*

Integrating out fast degrees of freedom is known to yield, to a good approximation, memory-less, i.e. Markovian, dynamics. In the presence of such a time-scale separation local detailed balance is believed to emerge and to guarantee thermodynamic consistency arbitrarily far from equilibrium. Here we present a transparent example of a Markov model of a molecular motor where local detailed balance can be violated despite a clear time-scale separation and hence Markovian dynamics. Driving the system far from equilibrium can lead to a violation of local detailed balance against the driving force. We further show that local detailed balance can be restored, even in the presence of memory, if the coarse-graining is carried out as Milestoning. Our work establishes Milestoning not only as a kinetically but for the first time also as a thermodynamically consistent coarse-graining method. Our results are relevant as soon as individual transition paths are appreciable or can be resolved.

The formulation of thermodynamic observables, such as heat and work, along individual stochastic trajectories unraveled fundamental fluctuation symmetries which matured into the framework called "stochastic thermodynamics" [1–3]. In the particular case of continuous-time Markov-jump processes the *local detailed balance* paradigm emerged, relating the kinetics to thermodynamic forces that drive a system out of equilibrium [2–5]. One inherent assumption of this paradigm is a separation of timescales [5]: the observed degrees of freedom are slow ensuring that all unobserved/hidden fast degrees of freedom equilibrate with instantaneously connected (heat or particle) reservoirs [3, 6, 7]. Accordingly, the forward and corresponding backward transition rates between a pair of meso-states A and B, $w_{A\to B}$ and $w_{B\to A}$, respectively, are related to the entropy production via [8]

$$k_{\mathrm{B}} \ln \frac{w_{A\to B}}{w_{B\to A}} = \text{entropy change } A \to B, \qquad (1)$$

where k_{B} is the Boltzmann constant, and the entropy difference reflects the change of both, the intrinsic entropy and the entropy generated in the reservoirs [5]. However, as soon as slow hidden degrees of freedom emerge (within A or B) the exact connection between the observed kinetics and the dissipation embodied in Eq. (1) disappears, which was explained theoretically [9–28] and corroborated experimentally [29]. The equality (1) can nevertheless be restored under specific conditions [13, 30–32], using affinities [33], by stalling the system [34, 35] or introducing waiting time distributions [27, 36–38] that *inter alia* can further trigger anomalous diffusion [39].

When the underlying degrees of freedom can assume continuous values any coarse-graining that lumps states as shown in Fig. 1a inherently leads to non-Markovian jump dynamics in continuous time [40, 41] due to fast re-crossings in the transition region between A and B. Notably, these can nowadays be experimentally resolved [42–47] and are therefore important practically. Conversely, *Milestoning* [48, 49] (see [50–52] for a broader perspective) turned out to be a coarse-graining scheme that allows for a kinetically consistent mapping of highdimensional dynamics onto a drastically simplified Markov-jump process [41, 53]. The state space is dissected into hypersurfaces which may enclose sub-volumes that are called "cores" [41, 53]. Fig. 1b depicts two such cores A and B, whereby the color of the trajectory encodes the last visited core. Beyond a short transient, Markov-jump dynamics emerges from the coarse-graining whenever the trajectory upon leaving any core either (i) quickly returns to it or (ii) quickly transits to the next core [41]. Hereby, condition (i) ensures a local equilibration prior to leaving a state that is required for the emergence of local detailed balance [2–5]. Besides being kinetically consistent, Milestoning offers two main advantages over lumping.

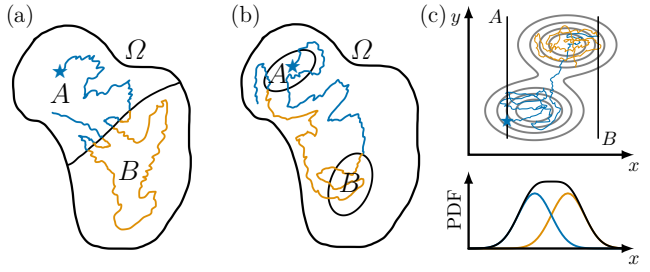

FIG. 1. Variants of coarse-graining: the color of the full trajectory evolving from the blue star represent the instantaneous coarse-grained states A (blue) and B (yellow), respectively. (a) State lumping: The full set of states Ω is decomposed into subsets A and B. (b) Milestoning based on core sets: two metastable states represent the cores A and B, and the coarse-grained state corresponds to the last visited core. (c) Top: contour lines depicting potential iso-surfaces in the xy plane; milestones A and B resolve the metastable regions. Bottom: measured equilibrium probability density function (PDF) with the PDFs of the the individual metastable states indicated in blue and orange, respectively.

First, in experiments probing low-dimensional observables one may be able to separate pairs of metastable states even if their projections onto the observable display an overlap (e.g., see [54]). This is illustrated in Fig. 1c, where two seemingly overlapping metastable states in the projected space x are resolved by choosing the respec-

tive milestones outside the overlapping region. Whenever a milestone is left, the trajectory rapidly returns or quickly transits to the other milestone. Thus, the last visited milestone to a good approximation reflects the currently visited metastable region in a possibly higher dimensional (here 2d) underlying space. Second, we recently discovered that Milestoning naturally ensures local detailed balance in the presence of a time scale separation [32]. Surprisingly, this extends even to systems without a clear time-scale separation, which we investigate further below. Notably, with so-called "dynamical coring" [54, 55] one can, under certain conditions, convert a "lumped" process into a "milestoned" process by manually discarding short recrossing events as those shown in Fig. 1a.

In contrast to continuous-space processes, the lumping of dynamics that evolve on a discrete state space [2–4, 6–10, 12–23, 27, 30, 31, 34–38] *can* in fact yield an effectively Markovian jump process. According to perturbation theory Eq. (1) is satisfied by lumped-state dynamics in the limit of an infinite time-scale separation [15], which was corroborated in [18, 19, 21]. This general belief was, however, never systematically scrutinized in practice.

In this Letter we show, by means of a simple yet biophysically relevant example, that time-scale separation surprisingly and against common belief does *not* ensure the existence of local detailed balance. The minimum time-scale separation required for Eq. (1) to hold may grow exponentially with the thermodynamic driving force. In other words, time-scale separation may not suffice *arbitrarily far* from equilibrium. Milestoning, in stark contrast to lumping (see Fig. 1), robustly ensures local detailed balance in the limit of a time-scale separation. This result indicates that unlike lumping, Milestoning generically yields a thermodynamically consistent coarse-graining.

F_1-ATPase driven far from equilibrium.— We consider the molecular motor F_1-ATPase driven by the hydrolysis of adenosine triphosphate (ATP). The dynamics evolves as a Markov processes on six rotational states [56] as shown in Fig. 2a: The binding of ATP occurs with a rate κ_+ proportional to the concentration of ATP and effetcs a 90° rotation. The reverse unbinding occurs with the rate κ_-. ATP hydrolisis to ADP is assumed to be infinitely fast. The release of ADP occurs with rate ω_+ and triggers a 30° rotation, and the reverse step occurs with rate ω_-.

The free energy μ liberated by the hydrolysis of one ATP $\to$ ADP at a given concentration relates to the entropy change times the temperature T, and local detailed balance (1) imposes

$$k_{\mathrm{B}}T \ln \frac{\omega_+\kappa_+}{\omega_-\kappa_-} = \mu. \tag{2}$$

Heneceforth we measure energies, μ, in units of the thermal energy $k_{\mathrm{B}}T$. The steady state probability to find the

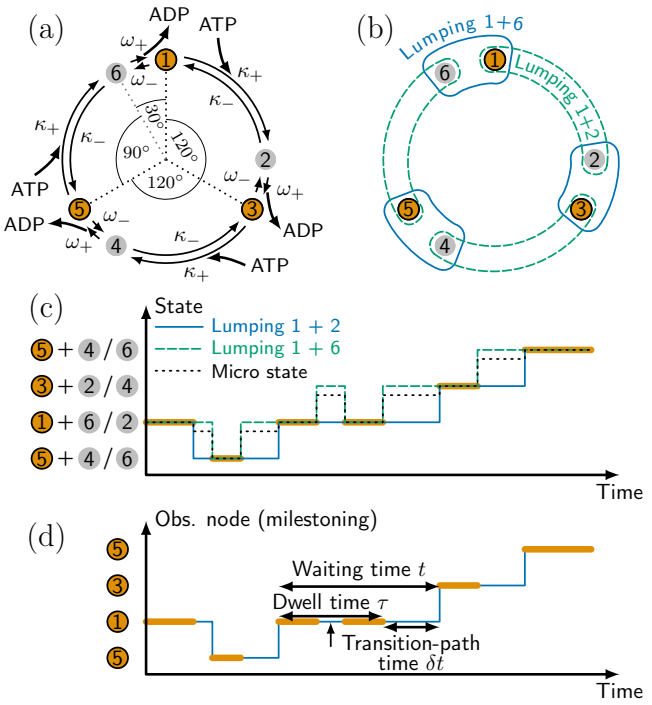

FIG. 2. Model and coarse-graining. (a) Full six state model; the dotted lines denote odd rotational states $\{1, 3, 5\}$ (orange) separated by 120°. The even intermediate states (gray) separate each rotation step into 90° and 30° substeps. (b) Two types of lumping; the solid boxes "lumping 1+6" lump states $\{1, 6\}$, $\{2, 3\}$, and $\{5, 6\}$, respectively, whereas the dashed boxes "lumping 1+2" lump states $\{1, 2\}$, $\{3, 4\}$, and $\{5, 6\}$. (c) Coarse-grained trajectory using "lumping 1+2" and "lumping 1+6"; the orange segments represent visits of odd states. The dotted line ("micro state") indicates the rotational state of the motor as function of time. (d) Coarse-grained trajectory deduced from Milestoning; the milestones are placed at odd states.

ATPase in even and odd states is given by [57]

$$P_{\mathrm{odd}} = \frac{\omega_+ + \kappa_-}{\omega + \kappa} \quad \text{and} \quad P_{\mathrm{even}} = \frac{\omega_- + \kappa_+}{\omega + \kappa}, \tag{3}$$

respectively, where we defined $\kappa \equiv \kappa_+ + \kappa_-$ and $\omega \equiv \omega_+ + \omega_-$. The entropy production rate can be expressed with the rate of ATP consumption, $J = P_{\mathrm{odd}}\kappa_+ - P_{\mathrm{even}}\kappa_-$, via [57]

$$\sigma = J\mu. \tag{4}$$

This completes the description of the "full" system.

Lumping.— We now perform a coarse-graining to reduce the six states to three. Two sensible ways to lump the states are shown in Fig. 2b. Assuming Markovian dynamics the effective forward "+" and backward "−" rates on the lumped space read [15]

$$\begin{aligned} W_\pm^{1+6} &= P_{\substack{\mathrm{odd}\\\mathrm{even}}}\kappa_\pm = \frac{(\omega_\pm + \kappa_\mp)\kappa_\pm}{\kappa + \omega}, \\ W_\pm^{1+2} &= P_{\substack{\mathrm{even}\\\mathrm{odd}}}\omega_\pm = \frac{(\omega_\mp + \kappa_\pm)\omega_\pm}{\kappa + \omega}, \end{aligned} \tag{5}$$

and satisfy $J = W_+^{1+6} - W_-^{1+6} = W_+^{1+2} - W_-^{1+2}$. In terms of effective rates the coarse-grained entropy reads [15]

$$\tilde{\sigma}_z = J \ln \frac{W_+^z}{W_-^z}, \tag{6}$$

with $z = 1+6$ or $z = 1+2$ and using Eqs. (4-6) yields

$$\frac{\tilde{\sigma}_{1+6}}{\sigma} = 1 - \frac{1}{\mu} \ln \frac{1 + \mathrm{e}^{\mu} \kappa_- / \omega_+}{1 + \kappa_- / \omega_+}, \tag{7}$$

$$\frac{\tilde{\sigma}_{1+2}}{\sigma} = 1 - \frac{1}{\mu} \ln \frac{1 + \mathrm{e}^{\mu} \omega_- / \kappa_+}{1 + \omega_- / \kappa_+}. \tag{8}$$

Both ratios (7) and (8) are positive and bounded by 1 [15], i.e., $\tilde{\sigma}_z \leq \sigma$ (see also [58]).

Time scale separation.— In agreement with [15] (see also [18, 19, 21]) in the limit $\kappa_- \ll \mathrm{e}^{-\mu}\omega_+$ (i.e., $\kappa \to 0$) we obtain $\tilde{\sigma}_{1+6} \approx \sigma$, whereas the limit $\omega_- \ll \mathrm{e}^{-\mu}\kappa_+$ (i.e., $\omega \to 0$) yields $\tilde{\sigma}_{1+2} \approx \sigma$. In other words, when hidden jumps are much faster than those between lumped states, the coarse-grained dynamics are approximately Markovian *and* preserve the entropy production.

In our model $\kappa \gg \omega$ and $\kappa \ll \omega$ are the only kinds of time scale separation, and in principle require two different types of lumping. At high ATP concentration ($\kappa \gg \omega$) "lumping $1+2$" (see dashed boxes in Fig. 2b) hides the fast degrees freedom $\sim \kappa$. Conversely, at low ATP concentration one should rather lump $1+6$ (see solid boxes in Fig. 2b). Note that whenever the entropy production rate is deduced from a master equation [2–4, 6–10, 12–23, 27, 28, 30, 31, 34–38] one explicitly (or implicitly) assumes the observed degrees of freedom to be formally infinitely slower than any possibly hidden ones.

Violation of local detailed balance.— In practice an infinite time-scale does not exist and the driving μ becomes important if it substantially exceeds the thermal energy ($\mu \gg 1$), which in turn implies $\mathrm{e}^{\mu} \ggg 1$. To see this set $\omega_\pm$ and κ_- to be constant while varying the ATP concentration as $\kappa_+ \propto e^{\mu}$ as in [56] (the parameters are given in Fig. 3). For $\mu < 10$ we find $\omega \gg \kappa$ and as expected $\tilde{\sigma}_{1+6} \approx \sigma$ (see Fig. 3). For $\mu > 15$ we have $\omega \ll \kappa$, however, to our surprise $\tilde{\sigma}_{1+2} \not\approx \sigma$ (because $\omega_- \not\ll \mathrm{e}^{-\mu}\kappa_+$). Inspecting Eq. (7) we actually find $\tilde{\sigma}_{1+2} \approx 1 - 10/\mu$ (see Fig. 3a). Thus one obtains $\tilde{\sigma}_{1+2}/\sigma \to 1$ in the limit $\mu \to 0$, which is approached algebraically slowly. For example, in the already unphysical situation $\mu = 40\, k_\mathrm{B}T$ [59] only 75 % of the entropy production are recovered in Eq. (6). Moreover, at physiological conditions $\mu = 20$ we find a clear time-scale separation, $\kappa/\omega \approx 140 \gg 1$, yet the entropy production is not even remotely restored. This surprising finding is the first main result of this Letter.

How can we reconcile this? For convenience we focus on $\mu = 20$ and the lumping "1+2", which in fact represents a semi-Markov process of second order [36] (see also [27, 37, 38]). That is, the waiting time density $\psi_{\pm|\pm}(t)$ depends on both, the previous and next visited state with

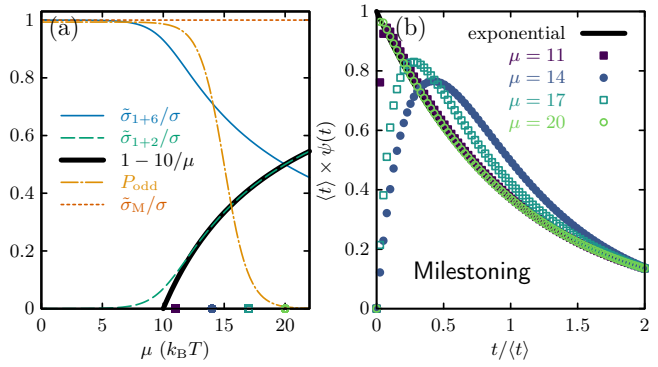

FIG. 3. Entropy production and waiting time statistics with Milestoning. (a) Entropy production, $\tilde{\sigma}_{1+6}$ and $\tilde{\sigma}_{1+2}$ deduced from the lumpings "1+6" and "1+2", respectively. The thick line depicting $1-10/\mu$ approaches $\tilde{\sigma}_{1+2}/\sigma$ in the limit $\mu \to \infty$. The dash-dotted yellow line denotes the steady state probability P_{odd}. (b) Probability density of waiting time t (see Fig. 2d) for μ values indicated in (a). The thick black line depicts an exponential density $\propto \mathrm{e}^{-t/\langle t \rangle}$. Parameters: $\omega_+ = 1$, $\omega_- = \mathrm{e}^{-5}$, $\kappa_+ = \mathrm{e}^{\mu-15}$, and $\kappa_- = \mathrm{e}^{-10}$.

the normalization $\int_0^\infty [\psi_{+|i}(t) + \psi_{-|i}(t)]dt = 1$ and $i = \pm$. In particular, for the given parameters we find

$$\begin{pmatrix} \psi_{+|+}(t) & \psi_{+|-}(t) \\ \psi_{-|+}(t) & \psi_{-|-}(t) \end{pmatrix} \approx \begin{pmatrix} 1.007 & 1.000 \\ 2.089 \cdot 10^{-9} & 2.075 \cdot 10^{-9} \end{pmatrix} \mathrm{e}^{-\lambda_1 t} + \begin{pmatrix} -1.007 & 3.100 \cdot 10^{-7} \\ 6.738 \cdot 10^{-3} & -2.075 \cdot 10^{-9} \end{pmatrix} \mathrm{e}^{-\lambda_2 t}, \tag{9}$$

where $\lambda_1 \approx 1.0$ and $\lambda_2 \approx 148.4$. The analytical expression for the waiting time density is immaterial for the present discussion but straightforward to determine. For times $t \gtrsim 0.15$ the jumps are essentially Markovian – the waiting time density is to a good approximation exponential and independent of the previous step, $\psi_{\pm|+} \approx \psi_{\pm|-}$, and the fast decaying mode is negligible, $\mathrm{e}^{-\lambda_2 t} \approx 0$. Hence, only short times $t \leq 0.15$ encode a violation of Markovianity. At strong driving most of the jumps occur in positive direction "+" and on average take equally long $\approx 1/\lambda_1 \approx 1$. In fact, only the backward jump "−" can be faster on average, however, if and only if the preceding jump occurred in the forward "+" direction, i.e. a forward transition is followed immediately by a backward transition. In this case one finds $\int_0^\infty t\psi_{-|+}(t)dt / \int_0^\infty \psi_{-|+}(t)dt \approx 0.0067 \approx 1/\lambda_2$. These rare events lead to an "overestimation" of the effective backward transition rate $W_-^{1+2} \gtrsim \omega_-\kappa_+/\kappa$. Note that a locally equilibrated backward rate would need to satisfy $\ln(W_-^{1+2}) \approx \ln(\omega_-\kappa_+/\kappa)$.

By evaluating exactly the waiting time distribution to include the short-time behavior one is able to restore the

entropy production from the two-step affinity via [36]

$$\sigma_{\rm aff}^{1+2} = J \ln \frac{\int_0^\infty \psi_{+|+}(t)dt}{\int_0^\infty \psi_{-|-}(t)dt} = J\mu, \tag{10}$$

where the last equality follows from Eqs. (2) and (9) (here $\mu = 20$). Thus, by taking into account the tiny non-Markovian features in Eq. (9) one can in principle recover the entropy production. This, however, poses a serious practical problem at strong driving $\mu \gg 1$. Namely, to deduce Eq. (10) from an experiment we formally require a trajectory with statistically sufficiently many incidents of finding *two consecutive backward steps not interrupted by a forward step*. It thus seems that one is required to reliably observe rare events with a probability $\propto (\mathrm{e}^{-\mu})^2$, which may not be feasible.

In the following we illustrate how an alternative coarse-graining – Milestoning – effectively restores Markovian dynamics in a thermodynamically consistent manner while it concurrently effectively squares the sample size by relying only on the evaluation of single rare backward jumps that occur with probability $\approx \mathrm{e}^{-\mu}$.

Thermodynamic consistency of Milestoning.— We define three milestones (or cores) at locations highlighted by dotted black lines in Fig. 1a. These represent the three odd rotational states. We measure the passages across the milestones (see thick yellow lines in Fig. 1c). If the angle were measured continuously, the passages through the milestones would correspond to instantaneous events [32]. The coarse-grained process at any time reflects the last visited Milestone (see blue line). As in Ref. [32] we dissect waiting times into the dwell and transition time periods. The dwell time represents all loops returning to the original milestone, while the transition-path time reflects the time of commuting between milestones. The waiting time can be shown to be the sum of the statistically independent dwell and transition-path times (see second main result in [32]). The main advantage of this decomposition is that the statistics of transition-path time encode information about potentially hidden multidimensional pathways [60] (see also [32, 61, 62]).

If the gaps between revisitations of the same milestone (see vertical arrow in Fig. 1d) *and* transition-path times are negligibly short compared to the waiting time in a state, the resulting "Milestoned process" becomes, to a good approximation, Markovian [41]. Note that milestones may represent closed (see [41] and Fig. 1b) or open (see [48, 49] and Fig. 1c) hypersurfaces.

Let $\phi_\pm$ denote the splitting probability that the next milestone will be visited in the forward "+" and backward "−" direction, respectively. One can confirm (cf. first main result in [32]) that

$$\ln \frac{\phi_+}{\phi_-} = \ln \frac{\kappa_+\omega_-}{\kappa_-\omega_-} = \mu \tag{11}$$

holds. That is, Milestoning transition probabilities *exactly* encode the entropy production per hydrolyzed ATP.

Since transition-path times obey a reflection symmetry [63] and because the dwell time statistics do not depend on the exit direction [32] the waiting time densities in the + and − direction coincide, i.e. $\psi_\pm(t) = \psi(t)$. In the presence of hidden dissipative mechanisms the symmetry may be lifted counterintuitively [64, 65]. Denoting the mean waiting time by $\langle t\rangle = \int_0^\infty t\psi(t)dt$, the steady state current becomes $J^{\rm M} = \phi_+/\langle t\rangle - \phi_-/\langle t\rangle = J$. Defining the Milestoning rates as $W_\pm^{\rm M} = \phi_+/\langle t\rangle$ and inserting them into Eq. (6) yields, using Eqs. (4) and (11), $\tilde\sigma_{\rm M} = \sigma$. Thus, Milestoning in contrast to lumping *preserves* the entropy production in the limit of a time-scale separation *and* beyond.

Upon inspecting the waiting time density we find that it is to a good approximation memory-less for $\mu \lesssim 10$ as well as for $\mu \gtrsim 20$, while the non-exponential behavior is most pronounced in the regime $10 \leq \mu \leq 20$ (see Fig. 3b). Thus, in the limit of either of the two time-scale separations, $\mu \lesssim 10$ and $\mu \gtrsim 20$, the Milestoned dynamics is to a good approximation Markovian. In contrast to lumping, Milestoning restores local detailed balance (1) in both directions, parallel and anti-parallel to the driving, even at large asymmetries, which is the second main result of this Letter.

Notably, the regime $\mu \lesssim 10$ clearly fulfills both criteria (i) and (ii) for the emergence of Markovian dynamics [41] if the probability to reside within a core satisfies $P_{\rm odd} \approx 1$. Conversely, the opposite limit $\mu \gtrsim 20$ does *not* obviously imply Markovian kinetics. To understand why it does so nevertheless, we point out that in this limit (a) $P_{\rm even} = 1 - P_{\rm odd} \approx 1$. If we were to choose the even (gray) states as cores instead of the odd (yellow) ones (see Fig. 2a), we would obviously restore the criteria for the emergence of Markovian dynamics [41]. It turns out further that (b) the waiting time density remains unaffected by the exchange of $\omega_\pm$ and $\kappa_\pm$, i.e. it does not depend on whether we choose the odd or even states as milestones. This explains why an exponential distribution emerges to a good approximation also in the limit $\mu \gtrsim 20$. We also note that the kinetic hysteresis discovered in [32] almost vanishes as soon as Markovian dynamics emerge *and* the aforementioned criteria [41] are satisfied, which here follows from (a) by choosing the even states as milestones.

Conclusion.— We have shown that a clear time scale separation, in contrast to the common belief, is only a necessary but *not* a sufficient condition for the validity of local detailed balance. By coarse-graining a detailed Markov model of a strongly driven molecular motor we demonstrated a clear time-scale separation between the observed and hidden degrees of freedom and hence Markovian dynamics of the observable, and concurrently the non-existence of a local equilibrium against the driving. Our work demonstrates, for the first time, that Milestoning restores thermodynamic consistency in the steady state in the presence of strong driving even if the dynamics displays memory. A coarse-graining not

based on Milestoning, e.g. lumping, may yield effectively Markovian dynamics that nevertheless violates local detailed balance. It will be interesting to revisit recent works on the thermodynamics of systems with slow hidden degrees of freedom that employed lumping [27, 36–38] to inspect if and how these change under the thermodynamically consistent Milestoning which will lead to correlated transitions [66] and/or dwell times [32].

Acknowledgments. The financial support from the German Research Foundation (DFG) through the Emmy Noether Program GO 2762/1-1 to A. G. is gratefully acknowledged.

* david.hartich@mpibpc.mpg.de
† agodec@mpibpc.mpg.de

[1] C. Jarzynski, Equalities and inequalities: Irreversibility and the second law of thermodynamics at the nanoscale, Annu. Rev. Condens. Matter Phys. **2**, 329 (2011).
[2] U. Seifert, Stochastic thermodynamics, fluctuation theorems and molecular machines, Rep. Prog. Phys. **75**, 126001 (2012).
[3] C. Van den Broeck and M. Esposito, Ensemble and trajectory thermodynamics: A brief introduction, Physica A **418**, 6 (2015).
[4] S. Katz, J. L. Lebowitz, and H. Spohn, Phase transitions in stationary nonequilibrium states of model lattice systems, Phys. Rev. B **28**, 1655 (1983).
[5] U. Seifert, Stochastic thermodynamics of single enzymes and molecular motors, Eur. Phys. J. E **34**, 26 (2011).
[6] K. Yoshimura and S. Ito, Information geometric inequalities of chemical thermodynamics, Phys. Rev. Res. **3**, 013175 (2021).
[7] K. Blom and A. Godec, Criticality in cell adhesion, Phys. Rev. X **11**, 031067 (2021).
[8] C. Maes, Local detailed balance, SciPost Phys. Lect. Notes , 32 (2021).
[9] S. Rahav and C. Jarzynski, Fluctuation relations and coarse-graining, J. Stat. Mech. , P09012 (2007).
[10] S. Pigolotti and A. Vulpiani, Coarse graining of master equations with fast and slow states, J. Chem. Phys. **128**, 154114 (2008).
[11] A. Gomez-Marin, J. M. R. Parrondo, and C. Van den Broeck, Lower bounds on dissipation upon coarse graining, Phys. Rev. E **78**, 011107 (2008).
[12] É. Roldán and J. M. R. Parrondo, Estimating dissipation from single stationary trajectories, Phys. Rev. Lett. **105**, 150607 (2010).
[13] A. Puglisi, S. Pigolotti, L. Rondoni, and A. Vupani, Entropy production and coarse graining in Markov processes, J. Stat. Mech. , P05015 (2010).
[14] É. Roldán and J. M. R. Parrondo, Entropy production and Kullback-Leibler divergence between stationary trajectories of discrete systems, Phys. Rev. E **85**, 031129 (2012).
[15] M. Esposito, Stochastic thermodynamics under coarse graining, Phys. Rev. E **85**, 041125 (2012).
[16] D. Andrieux, Bounding the coarse graining error in hidden Markov dynamics, Appl. Math. Lett. **25**, 1734 (2012).
[17] S. Bo and A. Celani, Entropy production in stochastic systems with fast and slow time-scales, J. Stat. Phys. **154**, 1325 (2014).
[18] G. Diana and M. Esposito, Mutual entropy production in bipartite systems, J. Stat. Mech. , P04010 (2014).
[19] A. C. Barato, D. Hartich, and U. Seifert, Efficiency of cellular information processing, New J. Phys. **16**, 103024 (2014).
[20] E. Zimmermann and U. Seifert, Effective rates from thermodynamically consistent coarse-graining of models for molecular motors with probe particles, Phys. Rev. E **91**, 022709 (2015).
[21] S. Bo and A. Celani, Multiple-scale stochastic processes: Decimation, averaging and beyond, Phys. Rep. **670**, 1 (2017).
[22] M. Kahlen and J. Ehrich, Hidden slow degrees of freedom and fluctuation theorems: an analytically solvable model, J. Stat. Mech. **2018**, 063204 (2018).
[23] M. Uhl, P. Pietzonka, and U. Seifert, Fluctuations of apparent entropy production in networks with hidden slow degrees of freedom, J. Stat. Mech. , 023203 (2018).
[24] A. Lapolla and A. Godec, Manifestations of projection-induced memory: General theory and the tilted single file, Front. Phys. **7**, 182 (2019).
[25] A. Lapolla and A. Godec, Single-file diffusion in a bistable potential: Signatures of memory in the barrier-crossing of a tagged-particle, J. Chem. Phys. **153**, 194104 (2020).
[26] A. Lapolla and A. Godec, Toolbox for quantifying memory in dynamics along reaction coordinates, Phys. Rev. Res. **3**, L022018 (2021).
[27] J. Ehrich, Tightest bound on hidden entropy production from partially observed dynamics, J. Stat. Mech. **2021**, 083214 (2021).
[28] B. Ertel, J. van der Meer, and U. Seifert, Operationally accessible uncertainty relations for thermodynamically consistent semi-Markov processes (2021), arXiv:2111.13113 [cond-mat.stat-mech].
[29] J. Mehl, B. Lander, C. Bechinger, V. Blickle, and U. Seifert, Role of hidden slow degrees of freedom in the fluctuation theorem, Phys. Rev. Lett. **108**, 220601 (2012).
[30] B. Altaner and J. Vollmer, Fluctuation-preserving coarse graining for biochemical systems, Phys. Rev. Lett. **108**, 228101 (2012).
[31] G. Teza and A. L. Stella, Exact coarse graining preserves entropy production out of equilibrium, Phys. Rev. Lett. **125**, 110601 (2020).
[32] D. Hartich and A. Godec, Emergent memory and kinetic hysteresis in strongly driven networks, Phys. Rev. X (in press); arXiv:2011.04628 (2021).
[33] F. Knoch and T. Speck, Cycle representatives for the coarse-graining of systems driven into a non-equilibrium steady state, New J. Phys. **17**, 115004 (2015).
[34] M. Polettini and M. Esposito, Effective thermodynamics for a marginal observer, Phys. Rev. Lett. **119**, 240601 (2017).
[35] G. Bisker, M. Polettini, T. R. Gingrich, and J. M. Horowitz, Hierarchical bounds on entropy production inferred from partial information, J. Stat. Mech. , 093210 (2017).
[36] I. A. Martínez, G. Bisker, J. M. Horowitz, and J. M. R. Parrondo, Inferring broken detailed balance in the ab-

sence of observable currents, Nat. Commun. **10**, 3542 (2019).
[37] D. J. Skinner and J. Dunkel, Improved bounds on entropy production in living systems, Proc. Natl. Acad. Sci. USA **118**, e2024300118 (2021).
[38] D. J. Skinner and J. Dunkel, Estimating entropy production from waiting time distributions, Phys. Rev. Lett. **127**, 198101 (2021).
[39] D. Hartich and A. Godec, Thermodynamic uncertainty relation bounds the extent of anomalous diffusion, Phys. Rev. Lett. **127**, 080601 (2021).
[40] M. Sarich, F. Noé, and C. Schütte, On the approximation quality of Markov state models, Multiscale Model. Simul. **8**, 1154 (2010).
[41] C. Schütte, F. Noé, J. Lu, M. Sarich, and E. Vanden-Eijnden, Markov state models based on milestoning, J. Chem. Phys. **134**, 204105 (2011).
[42] H. S. Chung, K. McHale, J. M. Louis, and W. A. Eaton, Single-molecule fluorescence experiments determine protein folding transition path times, Science **335**, 981 (2012).
[43] H. S. Chung and W. A. Eaton, Single-molecule fluorescence probes dynamics of barrier crossing, Nature **502**, 685 (2013).
[44] K. Neupane, D. B. Ritchie, H. Yu, D. A. N. Foster, F. Wang, and M. T. Woodside, Transition path times for nucleic acid folding determined from energy-landscape analysis of single-molecule trajectories, Phys. Rev. Lett. **109**, 068102 (2012).
[45] D. B. Ritchie and M. T. Woodside, Probing the structural dynamics of proteins and nucleic acids with optical tweezers, Curr. Opin. Struct. Biol. **34**, 43 (2015).
[46] K. Neupane, A. P. Manuel, and M. T. Woodside, Protein folding trajectories can be described quantitatively by one-dimensional diffusion over measured energy landscapes, Nat. Phys. **12**, 700 (2016).
[47] J.-Y. Kim and H. S. Chung, Disordered proteins follow diverse transition paths as they fold and bind to a partner, Science **368**, 1253 (2020).
[48] A. K. Faradjian and R. Elber, Computing time scales from reaction coordinates by milestoning, J. Chem. Phys. **120**, 10880 (2004).
[49] D. Shalloway and A. K. Faradjian, Efficient computation of the first passage time distribution of the generalized master equation by steady-state relaxation, J. Chem. Phys. **124**, 054112 (2006).
[50] R. Elber, D. E. Makarov, and H. Orland, *Molecular Kinetics in Condensed Phases: Theory, Simulation, and Analysis* (John Wiley & Sons, Ltd, 2020).
[51] R. Elber, Milestoning: An efficient approach for atomically detailed simulations of kinetics in biophysics, Annu. Rev. Biophys. **49**, 69 (2020).
[52] E. Suárez, R. P. Wiewiora, C. Wehmeyer, F. Noé, J. D. Chodera, and D. M. Zuckerman, What Markov state models can and cannot do: Correlation versus path-based observables in protein-folding models, J. Chem. Theory Comput. **17**, 3119 (2021).
[53] A. M. Berezhkovskii and A. Szabo, Committors, first-passage times, fluxes, Markov states, milestones, and all that, J. Chem. Phys. **150**, 054106 (2019).
[54] D. Nagel, A. Weber, B. Lickert, and G. Stock, Dynamical coring of Markov state models, J. Chem. Phys. **150**, 094111 (2019).
[55] A. Jain and G. Stock, Hierarchical folding free energy landscape of HP35 revealed by most probable path clustering, J. Phys. Chem. B **118**, 7750 (2014).
[56] R. Yasuda, H. Noji, M. Yoshida, K. Kinosita, and H. Itoh, Resolution of distinct rotational substeps by submillisecond kinetic analysis of F_1-ATPase, Nature **410**, 898 (2001).
[57] J. Schnakenberg, Network theory of microscopic and macroscopic behavior of master equation systems, Rev. Mod. Phys. **48**, 571 (1976).
[58] B. Nguyen, D. Hartich, U. Seifert, and P. De Los Rios, Thermodynamic bounds on the ultra- and infra-affinity of Hsp70 for its substrates, Biophys. J. **113**, 362 (2017).
[59] At physiological conditions $\mu \approx 20$ the ATP concentration is $c \sim 1\,\mathrm{mMol}$. Thus, $\mu = 40$ clearly corresponds to an unphysical ATP concentration of $c \sim 0.001\mathrm{e}^{20} \approx 500000\,\mathrm{Mol}$.
[60] R. Satija, A. M. Berezhkovskii, and D. E. Makarov, Broad distributions of transition-path times are fingerprints of multidimensionality of the underlying free energy landscapes, Proc. Natl. Acad. Sci. USA **117**, 27116 (2020).
[61] D. E. Makarov, Barrier crossing dynamics from single-molecule measurements, J. Phys. Chem. B **125**, 2467 (2021).
[62] A. M. Berezhkovskii and D. E. Makarov, On distributions of barrier crossing times as observed in single-molecule studies of biomolecules, Biophysical Reports , 100029 (2021).
[63] A. M. Berezhkovskii, G. Hummer, and S. M. Bezrukov, Identity of distributions of direct uphill and downhill translocation times for particles traversing membrane channels, Phys. Rev. Lett. **97**, 020601 (2006).
[64] J. Gladrow, M. Ribezzi-Crivellari, F. Ritort, and U. F. Keyser, Experimental evidence of symmetry breaking of transition-path times, Nat. Commun. **10**, 55 (2019).
[65] A. Ryabov, D. Lips, and P. Maass, Counterintuitive short uphill transitions in single-file diffusion, J. Phys. Chem. C **123**, 5714 (2019).
[66] A. T. Hawk and D. E. Makarov, Milestoning with transition memory, J. Chem. Phys. **135**, 224109 (2011).